Title page

Comparative Study of Trajectory Tracking Control for Automated Ground Vehicles via Model Predictive Control and Robust H-infinity State Feedback Control

Kai Yang is currently pursuing the Ph.D. degree in the *Department of Automotive Engineering, Chongqing University*, *Chongqing, China*. He received the B.E. degree in vehicle engineering from the *Wuhan University of Technology*, in 2018.
E-mail: kaiyang0401@gmail.com

Xiao-Lin Tang is currently an Associate Professor at the *Department of Automotive Engineering, Chongqing University,* Chongqing, China. He received the Ph.D. degree in Mechanical Engineering from *Shanghai Jiao Tong University*, *China*, in 2015.
E-mail: tangxl0923@cqu.eud.cn

Ye-Chen Qin is currently working as an Associate Professor with the *Beijing Institute of Technology, China*. He received the B.Sc. and Ph.D. degrees in mechanical engineering from the *Beijing Institute of Technology, China*, in 2010 and 2016, respectively.
E-mail: qinyechenbit@gmail.com

Yan-Jun Huang is currently a Research Associate at the Department of Mechanical and Mechatronics Engineering at *University of Waterloo*, where he received his PhD degree in 2016.
E-mail: y269huan@uwaterloo.ca

Hong Wang is currently a Research Associate in mechanical and mechatronics engineering with the *University of Waterloo*. She received the Ph.D. degree from the *Beijing Institute of Technology, China,* in 2015.
E-mail: hong.wang@uwaterloo.ca

Hua-Yan Pu, is currently a Professor at State Key Laboratory of Mechanical Transmissions, Chongqing University, Chongqing, China. She received the Ph.D. degree from the *Huazhong University of Science and Technology, China,* in 2011.
E-mail: phygood 2001@shu.edu.cn

Corresponding author：Xiao-Lin Tang　E-mail：tangxl0923@cqu.eud.cn

ORIGINAL ARTICLE

Comparative Study of Trajectory Tracking Control for Automated Ground Vehicles via Model Predictive Control and Robust H-infinity State Feedback Control

Kai Yang[1] • Xiao-Lin[1]* • Ye-Chen Qin[2] • Yan-Jun Huang[3] • Hong Wang[4] • Hua-Yan Pu[1]

Received June xx, 201x; revised February xx, 201x; accepted March xx, 201x

Abstract: A comparative study of longitudinal and lateral control maneuverer in model predictive control (MPC) schemes and robust H_∞ state feedback control (RSC) method for trajectory tracking of automated ground vehicles (AGVs) is presented in this paper. Both MPC-based and RSC-based tracking controller are designed on the same basis of longitudinal-lateral-yaw motions of a single-track vehicle model. The main objective is to compare the controllers' performance of tracking accuracy of path and velocity under different test scenarios. The simulation is implemented on Carsim-Simulink joint platform using high-fidelity vehicle model and the mass uncertainties, sensor measurement noise and the performance in extreme driving conditions: 90° turn with big curvature are considered. The simulation results indicate that mass uncertainty and sensor measurement noise of lateral velocity have little effect on the RSC-based controller, while that have relatively great influence on MPC-based one. However, MPC-based controller shows a shorter response time and more accurate tracking performance than RSC-based scheme. Finally, for the test of 90° turn with curvature $0.02m^{-1}$, the maximum velocity that RSC-based controller can carry out has reached 22m/s, which is slightly better than MPC-based one: 21m/s.

Keywords: Trajectory tracking • Automated ground vehicles • Model predictive control • Robust H_∞ state feedback control

1 Introduction

The increasing demands on mobility, efficiency and safety have extremely promoted the development of intelligent transportation system (ITS) in recent years [1]. As one of the most promising technologies of automotive industry, automated ground vehicles (AGVs) with the improved security and better road utilization have many potential applications in many fields and have attracted many attentions from both industry and academic communities [2-3]. Generally, the typical architecture of an AGV system mainly incorporates two parts [4-6], namely, perception system and decision-making and each of them is generally divided into many subsystems that are shown in Figure 1. Trajectory tracking control is a fundamental issue for AGVs, which is devoted to track a predefined path and velocity profiles accurately and the errors (i.e. the lateral offset, heading and velocity errors) need to converge to zero during the manipulating process [7].

In recent years, much research work on trajectory tracking have been studied [8-13] and the main challenges of achieving accurate trajectory tracking lie in the following aspects: (1) non-holonomic property and multi-constrains of AGVs; (2) trade-off between vehicle model accuracy and computation efficiency; (3) uncertainties and time-varying parameters of vehicle dynamic model; (4) external disturbances of complex driving environment. Besides, the interaction between road and tires is also an important source of coupling. According to the vehicle dynamics, it's known that the maximal longitudinal and lateral tire force is determined based on the friction ellipse under certain road conditions [14]. Furthermore, for most existing literatures of trajectory tracking, the bicycle vehicle model which describes longitudinal, lateral and yaw motion is usually adopted for the controller design. But owing to the yaw motion caused by wheels steering, different dynamic and kinematic couplings can put huge impact on the controllers' performance [15]. It's well known that model predictive control and robust H_∞ control theory are two effective techniques to address the problems mentioned above [16-20]. Figure 2 illustrates the research trend of trajectory

✉ Xiao-Lin Tang
tangxl0923@cqu.eud.cn

1 State Key Laboratory of Mechanical Transmissions, College of Automotive Engineering, Chongqing University, Chongqing, China;

2 School of Mechanical Engineering, Beijing Institute of Technology, Beijing, China;

3 Department of Mechanical and Mechatronics Engineering, University of Waterloo, Waterloo, Canada;

4 School of Vehicle and Mobility, Tsinghua University, Beijing, China.

tracking using MPC and robust H_∞ control method of AGVs, which is derived by using keywords like 'trajectory tracking MPC' and 'trajectory tracking Robust H_∞ control' to find the number of papers published in this fields from 2000 to 2019 in Web of Science.

On the one hand, MPC has become one of the most popular optimal control methods in these years due to its well performance in processing multi-constrained linear or non-linear system [21-22] and it is easy to be used at different levels of the process control structure and offers attractive solutions for tracking problems while guaranteeing stability [23-24]. Owing to its advantages, MPC has been widely implemented in autonomous industry including trajectory tracking issues. For example, the trajectory controller is usually designed by formulating the tracking task as a multi-constrained model predictive control (MMPC) [25-29]. In one word, MPC uses a mathematical dynamic process model to predict future system states and gets the optimal control values by formulating trajectory tracking issues as an optimal control problem and solving it with effective optimal algorithm. On the other hand, robust H_∞ control has certain advantages in handling the presence of model uncertainties and external disturbances, which may result from variations of vehicles or environment parameters as well as the vehicle states [7]. Ref [30] manages to devise a robust H_∞ path following control strategy for AGVs with considering signal transmission delay and data dropouts. In addition, the time-varying parameters, steering system backlash-type hysteresis, and uncertainties of nonlinear tire model are also considered in [31-33]. In short, the aim of robust H_∞ control law is to design the feedback gain of the controller, which can make the system's output of external disturbance is as small as possible under the presence of model uncertainties.

Though MPC and robust H_∞ control are two effective strategies in tackling trajectory tracking issues, they show many differences in some aspects. For instance, robust H_∞ control does not consume too much on-board computation resources as its feedback gain is usually calculated offline, whereas MPC needs to solve complex optimization problems in order to get the optimal control values online. Therefore, the objective of this paper is to systematically compare the practicality of MPC method and robust H_∞ state feedback control (RSC) approach when considering mass uncertainties, sensor measurement noise and the performance in extreme driving conditions. To the best of the present authors' knowledge, there has no comparative study of trajectory tracking control with MPC and RSC techniques. The main contribution of this paper is to evaluate MPC-based and RSC-based trajectory tracking controllers' performance and show their advantages and disadvantages with respect to robustness to parameters uncertainties and extreme driving conditions. In order to carry out a fair comparation between MPC and RSC, some details need to be explained in advance. Specifically, the most important performance index of controllers in this paper is tracking accuracy while satisfying system constrains. Besides, they both utilize the same tracking error model on account of combined longitudinal-lateral-yaw dynamic vehicle model to design control laws. Furthermore, the adjustable parameters of both controllers are obtained through trial and error method, trying to ensure that controllers can achieve optimal control performance (i.e. prediction horizon N_p of MPC).

The rest of the paper are organized as follows. In section 2, the trajectory tracking error model and combined longitudinal-lateral-yaw vehicle dynamics model are deduced. In section 3, the controllers based on MPC and RSC are designed to track path and velocity profiles, respectively. Then, the performance of MPC-based and RSC-based controllers is demonstrated by testing them in jointed Carsim-Simulink platform with the respect to parameter uncertainties and extreme driving condition in section 4 and finally, the conclusions are illustrated in section 5.

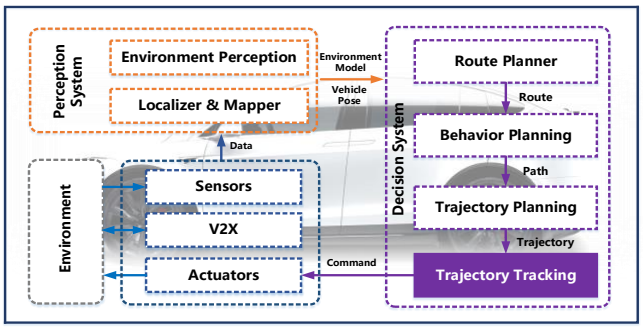

Figure 1 Overview of the typical architecture of AGVs

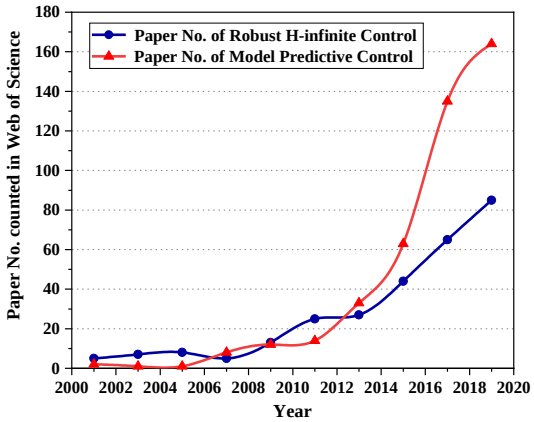

Figure 2 Research trend of trajectory tracking using Robust H_∞ control and MPC

2 Trajectory Tracking and 3-DOF Vehicle Dynamic Model of AGVs

2.1 Trajectory Tracking Model

The trajectory tracking model is shown in Figure 3 and the definition of parameters used in this paper is shown in Table 1. At any given time, we assume that the reference point is given by a tuple $[x_r, y_r, \varphi_r, v_r]^T$ and subscript r represents the variables which are defined by reference profiles. As shown in Figure 3, the lateral offset e_y can be calculated by:

$$e_y = (x - x_r)\sin(\varphi_r) - (y - y_r)\cos(\varphi_r) \quad (1)$$

The heading error e_φ and velocity error e_v are defined as follows

$$\begin{cases} e_\varphi = \varphi - \varphi_r \\ e_v = v_x - v_r \end{cases} \quad (2)$$

Given the road curvature C_R, the desired yaw rate is obtained:

$$\dot{\varphi}_r = v_x C_R \quad (3)$$

Besides, the derivatives of CG's positon can be obtained from the kinematic relationship:

$$\begin{cases} \dot{x} = v_x\cos(\varphi) - v_y\sin(\varphi) \\ \dot{y} = v_x\sin(\varphi) + v_y\cos(\varphi) \end{cases} \quad (4)$$

Thus, combined equation (1) with (2)-(4), we can get

$$\begin{cases} \dot{e}_y = \dot{x}sin(\varphi_r) - \dot{y}\cos(\varphi_r) = v_x\sin(e_\varphi) + v_y\cos(e_\varphi) \\ \dot{e}_\varphi = r - v_x C_R \\ \dot{e}_v = \dot{v}_x - \dot{v}_r \end{cases} \quad (5)$$

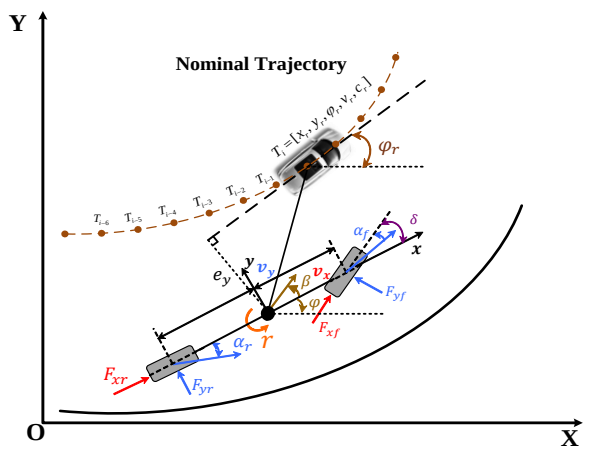

Figure 3 Schematic diagram of trajectory tracking model and vehicle dynamic model

Table 1 Symbol and definition of the tracking system

Parameters	*Unit*	*Description*
x/y	m	Coordinates of center of gravity (CG)
φ	rad	Yaw angle of vehicle body (in inertial coordinates system, OXY)
r	rad/s	Yaw rate of vehicle body
v_x/v_y	m/s	Longitudinal/Lateral velocity (in local coordinates system, oxy)
e_y	m	Offset of CG from the reference point
e_φ	rad	Orientation error of yaw angle with respect to the reference trajectory
e_v	m/s	Error between the current and the desired longitudinal velocity
m	kg	Vehicle mass
I_Z	$kg \cdot m^2$	Yaw moment of inertia of the vehicle
l_f/l_r	m	Distance from CG to the front/ real axle
F_{xf}/F_{xr}	N	Longitudinal tire force of the front/rear wheel
F_{yf}/F_{yr}	N	Lateral tire force of the front/rear wheel
C_f/C_r	N/rad	Cornering stiffness of the front/real wheel
α_f/α_r	rad	Slip angle of the front/ rear wheel
F_x	N	Generalized longitudinal force
δ_f	rad	Front wheel steering angle
C_R	m^{-1}	Road curvature

2.2 3-DOF Vehicle Dynamic Model

The schematic diagram of single-track vehicle model coupled 3-DOF (degree of freedom) vehicle dynamic model is also shown in Figure 3. According to Newton's laws, the vehicle's dynamics in the yaw plane can be described by the differential equations:

$$\begin{cases} m(\dot{v}_x - rv_y) = F_{xf} + F_{xr} = F_x \\ m(\dot{v}_y + v_x r) = F_{yf} + F_{yr} \\ I_z\dot{r} = l_f F_{yf} - l_r F_{yr} \end{cases} \quad (6)$$

where F_x means the generalized longitudinal force of AGVs including wind drag and tire rolling resistance. And the front and rear lateral force F_{yf} and F_{yr} are the function of tire slip angles and can be calculated as follows

$$F_{yf} = C_f\alpha_f,\ F_{yr} = C_r\alpha_r \quad (7)$$

where α_f and α_r denote the wheel slip angles, which can be obtained as

$$\alpha_f = \delta_f - \frac{l_f\dot{r} + v_y}{v_x},\ \alpha_r = \frac{l_r\dot{r} - v_y}{v_x} \quad (8)$$

Therefore, combined equation (6) with (7) and (8), we have

$$\begin{cases} \dot{v}_y = a_{11}v_y + a_{12}r + b_1\delta_f \\ \dot{r} = a_{21}v_y + a_{22}r + b_2\delta_f \\ \dot{e}_y = v_x sine_\varphi + v_y cose_\varphi \\ \dot{e}_\varphi = r - C_R(e_v + v_{xr}) \\ \dot{e}_v = rv_y + \dot{v}_{xr} + F_x/m \end{cases} \quad (9)$$

where $a_{11} = -\frac{(C_f+C_r)}{mv_x}$, $a_{12} = -v_x - \frac{(l_fC_f-l_rC_r)}{mv_x}$, $a_{21} = -\frac{(l_fC_f-l_rC_r)}{I_zv_x}$, $a_{22} = -\frac{\left(l_f^2C_f+l_r^2C_r\right)}{I_zv_x}$, $b_1 = \frac{C_f}{m}$, $b_2 = \frac{l_fC_f}{I_z}$.

In order to facilitate the controller design, rewrite the equation (9) to form the following linear state-space equation, which can be represented as:

$$\begin{cases} \dot{x}(t) = A(t)x(t) + B(t)u(t) + D(t) \\ y(t) = C(t)x(t) \end{cases} \quad (10)$$

with $A(t) = \begin{bmatrix} a_{11} & a_{12} & 0 & 0 & 0 \\ a_{21} & a_{22} & 0 & 0 & 0 \\ 1 & 0 & 0 & v_x & 0 \\ 0 & 1 & 0 & 0 & -C_R \\ r & 0 & 0 & 0 & 0 \end{bmatrix}$, $B(t) = \begin{bmatrix} 0 & b_1 \\ 0 & b_2 \\ 0 & 0 \\ 0 & 0 \\ 1/m & 0 \end{bmatrix}$, $D(t) = \begin{bmatrix} 0 \\ 0 \\ 0 \\ -C_Rv_x \\ -\dot{v}_r \end{bmatrix}$, $C(t) = \begin{bmatrix} 0 & 1 & 0 & 0 & 0 \\ 0 & 0 & 1 & 0 & 0 \\ 0 & 0 & 0 & 1 & 0 \\ 0 & 0 & 0 & 0 & 1 \end{bmatrix}$

where the state variables is $x(t) = \left[v_y, r, e_y, e_\varphi, e_v\right]^T$ and the output variables is $y(t) = [r, e_y, e_\varphi, e_v]^T$. The control input is the front wheel steering angle δ_f and the generalized longitudinal tire force F_x, namely, $u(t) = \left[F_x, \delta_f\right]^T$ and $D(t)$ is disturbance.

3 Control Law Allocation

3.1 Trajectory Tracking Controller Based on MPC

3.1.1 Formulation of Augmented System

As analyzed above, the trajectory tracking task can be posed as predictive control problem with multi-constraints. Note that the model described in equation (10) is a linearized and continuous-time system. To facilitate MPC controller design, the continuous-time system needs to be transformed into discrete state-space mode with the fixed sampling period T. Here, the zero-order hold (ZOH) method [11] is applied and the equation (10) can be depicted as discrete form:

$$\begin{cases} x(k+1) = A_dx(k) + B_du(k) + D(k) \\ y(k+1) = C_dx(k) \end{cases} \quad (11)$$

where $A_d \in R^{5\times5}, B_d \in R^{5\times2}$ and $C_d \in R^{4\times5}$ are the system coefficient matrices and k means the time step.

Furthermore, to achieve a better control performance, the state vector $x(k)$ and the increment input $\Delta u(k)$ are usually coupled in an augmented vector, which can be represented as $\tilde{x}(k) = [x(k),\ \Delta u(k)]^T$. And the control input can be calculated by

$$u(k) = u(k-1) + \Delta u(k) \quad (12)$$

Thus, the system equations (11) can be rewritten as the following equations:

$$\begin{cases} \tilde{x}(k+1) = \tilde{A}(k)\tilde{x}(k) + \tilde{B}(k)\Delta u(k) + \widetilde{D}(k) \\ \tilde{y}(k+1) = \tilde{C}(k)\tilde{x}(k) \end{cases} \quad (13)$$

where $\tilde{A}(k) = \begin{bmatrix} A_d & B_d \\ 0_{2\times5} & I_2 \end{bmatrix}$, $\tilde{B}(k) = \begin{bmatrix} B_d \\ I_2 \end{bmatrix}$ and $\tilde{C}(k) = [C_d \quad 0_{4\times2}]$.

Using the physical model to predict the future behavior of system is one of the most important processes in MPC controller design. The prediction horizon N_p and control horizon N_c need to be defined and the value is determined by considering the tracking accuracy and time efficiency. The sequence of future incremental inputs and disturbances at time step k are denoted as $\Delta U(k)$ and $\overline{D}(k)$, respectively.

$$\begin{cases} \Delta U(k) = [\Delta u(k), \Delta u(k+1), \cdots, \Delta u(k+N_c-1)]^T \\ \overline{D}(k) = [\widetilde{D}(k), \widetilde{D}(k+1), \cdots, \widetilde{D}(k+N_p-1)]^T \end{cases} \quad (14)$$

Therefore, the predicted output can be calculated by the following formulations:

$$\begin{cases} \tilde{x}(k+1) = \tilde{A}\tilde{x}(k) + \tilde{B}\Delta u(k) + \widetilde{D}(k) \\ \tilde{x}(k+2) = \tilde{A}^2x(k) + \tilde{A}\tilde{B}\Delta u(k) + \tilde{A}\widetilde{D}(k) + \tilde{B}\Delta u(k+1) \\ \qquad\qquad \vdots \\ \tilde{x}(k+N_c) = \tilde{A}^{N_c}x(k) + \tilde{A}^{N_c-1}\tilde{B}\Delta u(k) + \tilde{A}^{N_c-1}\widetilde{D}(k) + \\ \qquad\qquad +\tilde{B}\Delta u(k+N_c-1) + \widetilde{D}(k+N_c-1) \\ \qquad\qquad \vdots \\ \tilde{x}\left(k+N_p\right) = \tilde{A}^{N_p}x(k) + \tilde{A}^{N_p-1}\tilde{B}\Delta u(k) + \tilde{A}^{N_p-1}\widetilde{D}(k) + \cdots + \\ \qquad \tilde{A}^{N_p-N_c}\tilde{B}\Delta u(k+N_c-1) + \tilde{A}^{N_p-N_c}\widetilde{D}(k+N_c-1) \\ \qquad + \cdots \widetilde{D}\left(k+N_p-1\right) \end{cases} \quad (15)$$

Here, we define the predicted outputs of the predictive state-space model at time step k as:

$$Y(k) = [\tilde{y}(k+1), \tilde{y}(k+2), \cdots, \tilde{y}(k+N_p)]^T \quad (16)$$

Denote the performance outputs over the prediction horizon N_p as a compact matrix form:

$$Y(k) = \Gamma\tilde{x}(k) + \Theta\Delta U(k) + \xi\overline{D}(k) \quad (17)$$

with $\Gamma = [\tilde{C}\tilde{A}, \tilde{C}\tilde{A}^2, \cdots \tilde{C}\tilde{A}^{N_c}, \cdots, \tilde{C}\tilde{A}^{N_p}]^T$,

$$\Theta=\begin{bmatrix}\tilde{C}\tilde{B} & 0 & \cdots & 0\\ \tilde{C}\tilde{A}\tilde{B} & \tilde{C}\tilde{B} & \cdots & \vdots\\ \vdots & \vdots & \cdots & 0\\ \tilde{C}\tilde{A}^{N_c-1}\tilde{B} & \tilde{C}\tilde{A}^{N_c-2}\tilde{B} & \cdots & \tilde{C}\tilde{B}\\ \vdots & \vdots & \ddots & \vdots\\ \tilde{C}\tilde{A}^{N_c-1}\tilde{B} & \tilde{C}\tilde{A}^{N_c-2}\tilde{B} & \cdots & \tilde{C}\tilde{A}^{N_p-N_c}\tilde{B}\end{bmatrix}$$

$$\xi=\begin{bmatrix}\tilde{C} & 0 & \cdots & 0\\ \tilde{C}\tilde{A} & \tilde{C} & \cdots & 0\\ \tilde{C}\tilde{A}^2 & \tilde{C}\tilde{A} & \cdots & 0\\ \vdots & \vdots & \ddots & \vdots\\ \tilde{C}\tilde{A}^{N_p-1} & \tilde{C}\tilde{A}^{N_p-2} & \cdots & \tilde{C}\end{bmatrix}$$

3.1.2 Formulation of Trajectory Tracking Problem Using MPC

The aim of MPC-based trajectory tracking controller is to make the predicted outputs as close as possible to the reference trajectory within the predictive horizon, and the reference trajectory $Y_r(k)$ is assumed to remain unchanged during an optimization window. The reference signals are described as:

$$Y_r(k)=[\tilde{y}_r(k+1),\tilde{y}_r(k+2),\cdots,\tilde{y}_r(k+N_p)]^T \quad (18)$$

Thus, a typical tracking accuracy and control smoothness-oriented cost function over the predictive horizons is defined:

$$\mathcal{L}\big(x,u(k-1),U(k)\big)=\min_{\Delta U_k}\{[Y_r(k)-Y(k)]^T\bar{Q}[Y_r(k)-Y(k)]+\Delta U^T(k)\bar{R}\Delta U(k)\} \quad (19)$$

where diagonal matrices $\bar{Q}$ and $\bar{R}$ are the positive definite weight matrices (i.e. $\bar{Q}>0$ and $\bar{R}>0$) which can be regulated to achieve desired closed-loop performance. The first item in cost function reflects the tracking error between the predictive outputs and the reference trajectory. The second one refers to the penalty on the control inputs that is to make the control process smoother.

So far, the main task has converted to find an optimal control inputs $\Delta U(k)$ that can minimize the cost function $\mathcal{L}(x,u)$. However, AGVs have many inherent physical limitations needed to be taken into accounted. Specifically, these limitations on the capacity of control actuators or on the rate of control actuators result in the hard constrains of the trajectory tracking system. Besides, there are also some restrictions imposed on output variables due to environment conditions (i.e. road boundary, speed limit, etc.). Each type of constrains can make huge difference on the performance of the tracking system including the stabilization. According to the kinematics and dynamics of the vehicle model, the constrains for this trajectory tracking problem are specified as:

$$\begin{cases}\Delta U_{\min}(k)\le\Delta U(k)\le\Delta U_{max}(k)\\ U_{\min}(k)\le G\Delta U+Fu(k-1)\le U_{max}(k)\\ Y_{min}\le Y(k)\le Y_{max}\end{cases} \quad (20)$$

with

$$G=\begin{bmatrix}1 & 0 & \cdots & 0 & 0\\ 1 & 1 & \cdots & 0 & 0\\ 1 & 1 & \ddots & \vdots & \vdots\\ 1 & 1 & \cdots & 1 & 0\\ 1 & 1 & \cdots & 1 & 1\end{bmatrix}_{N_c\times N_c}\qquad F=\begin{bmatrix}1\\1\\\vdots\\1\\1\end{bmatrix}_{1\times N_c}$$

where $\Delta U_{\min}$, ΔU_{max}, $U_{\min}$, $U_{max}\in R^{2N_c\times 1}$, Y_{min}, $Y_{max}\in R^{4\times 1}$ and $u(k-1)$ is the control inputs at time *k-1*.

The first and second inequality are adopted to prevent aggressive control strategy and avoid actuator saturation, respectively, and the third one is imposed to restrict output variables. Then, combined equation (19) with (20), the trajectory tracking problem is converted to solve the following optimal problem with multi-constrains:

$$\mathcal{L}\big(x,u(k-1),U(k)\big)=$$

$$\min_{\Delta U_k}\{[Y_r(k)-Y(k)]^T\bar{Q}[Y_r(k)-Y(k)]+\Delta U^T(k)\bar{R}\Delta U(k)\}$$

$$s.t.\begin{cases}\Delta U_{\min}\le\Delta U\le\Delta U_{max}\\ U_{\min}\le G\Delta U+Fu(k-1)\le U_{max}\\ Y_{min}\le Y(k)\le Y_{max}\end{cases} \quad (21)$$

It's found that the optimization problem (21) is based on linear system and the cost function is convex quadratic that means it's can be remade as quadratic program issues (QP) if the constrains are convex too. The problem described in equation (21) needs to be translated into standard form of quadratic problems:

$$\mathcal{L}'\big(x,u(k-1),U(k)\big)=\min_{\Delta U_k}\left\{\frac{1}{2}\Delta U^T(k)G_k\Delta U(k)+\mathrm{C}^T\Delta U(k)\right\}$$
$$s.t.\begin{cases}\Delta U_{\min}\le\Delta U\le\Delta U_{max}\\ U_{\min}\le G\Delta U+Fu(k-1)\le U_{max}\\ Y_{min}\le Y(k)\le Y_{max}\end{cases} \quad (22)$$

where $G_k=2(\Theta^T\bar{\mathrm{Q}}\Theta+\bar{\mathrm{R}})$, $C=\Theta^T\bar{\mathrm{Q}}(\Gamma\tilde{x}-Y_r+\xi\bar{D})$.

Then, at time step k, the above quadratic problem can be solved (i.e. quadprog function in Matlab) and will get a solution ΔU_k^*. Once the solution is obtained, the first element of solution vector in vector, namely, Δu_k^* will be used and the optimal control inputs at this time step is computed as:

$$u(k)=u(k-1)+\Delta u_k^* \quad (23)$$

Similarly, at next time step $k+1$, new input measurements and updated system states produce new

quadratic problem that needs to solve. In conclusion, by solving a quadratic problem at each time step, the MPC controller will get an optimal input for next time step. However, in most cases, there are some non-convex constrains need to process and the SCFS method in [34] can be used to convert the optimal problem with non-convex constrains to with convex constrains equivalently.

3.2 Trajectory Tracking Controller Based on RSC

3.2.1 Preliminary Knowledge of RSC

We re-emphasize that the main objective of this paper is a comparative study of path-following control of an AGV employing different control strategies. Both MPC-based and RSC-based tracking controllers use standard design methods, and specifically, the RSC-based tracking controller design mainly adopts the theory applied in the literature [7][20]. To carry out a fair comparison of tracking responses with those from MPC, RSC is also based on the linearized vehicle model (10) and the general objective function is as follows

$$\int_0^t y^T(t)\, y(t)dt \le \gamma^2 \int_0^t D^T(t)\, D(t)dt \tag{24}$$

where the main task is to obtain a control law that can make the closed-loop system satisfy the asymptotically stability and fulfill the H_∞ performance index γ that attenuate the effect of the external disturbance $D(t)$.

Before the controller design, some essential lemmas and theorems also need to be introduced. Consider a polytopic LPV (linear parameter-varying) system which is described by state-space equations as follows:

$$\begin{cases} \dot{x}(t) = A_0(q)x(t) + B_0(q)u(t) \\ y(t) = C_0(q)x(t) \end{cases} \tag{25}$$

And it's equal to the following equations

$$\begin{cases} \dot{x}(t) = \sum_{i=1}^{n} q_i \left[A_{0i}x(t) + B_{0i}u(t)\right] \\ y(t) = \sum_{i=1}^{n} q_i\, C_{0i}x(t) \\ \sum_{i=1}^{n} q_i = 1\,,\ q_i \ge 0 \end{cases} \tag{26}$$

where the A_{0i}, B_{0i} and C_{0i} are the values of $A_0(q)$, $B_0(q)$ and $C_0(q)$ at the vertex q_i of the parameters polytope.

Theorem 1: Given a positive scalar γ_0, the system described in equation (26) is asymptotically stable and meets the H_∞ performance index (24), if and only if there exists n symmetric definite matrices P_i and a matrix S_0 satisfying the following conditions

$$\begin{bmatrix} A_{0i}S_0 + S_0^T A_{0i}^T & S_0^T B_{0i}^T & C_{0i} & P_i - S_0^T \\ * & -\gamma_0 I & 0 & 0 \\ * & * & -\gamma_0 I & 0 \\ * & * & * & 0 \end{bmatrix} < 0, i = 1,2,\cdots n \tag{27}$$

The proof of this theorem can be found in [20]. The RSC-based controller design is on account of linear matrix inequality (LMI) method. So far, the preliminary knowledge has been prepared sufficiently for the RSC-based controller design.

3.2.2 Formulation of trajectory tracking problem

Similar to MPC-based controller, the constrains imposed on inputs should be taken into consideration [35]. Define as following Lyapunov equation

$$V(t) = x(t)^T P x(t) \tag{28}$$

and assume the following condition is satisfied

$$x(t)^T P x(t) < \eta \tag{29}$$

$$u(t) = Kx(t) \tag{30}$$

where K is the gain of the controller and η is a given constant. The maximum inputs are denoted as u_{max}, then,

$$max\|u(t)\|^2 = max\|x^T(t)K^T K x(t)\|$$

$$= max\left\|x^T(t)P^{\frac{1}{2}}P^{-\frac{1}{2}}K^T K P^{-\frac{1}{2}}P^{\frac{1}{2}}x(t)\right\|$$

$$< \eta\theta_{max}(P^{-\frac{1}{2}}K^T K P^{-\frac{1}{2}}) \le u_{max}I \tag{31}$$

where θ_{max} is the largest eigenvalue of the matrix $(P^{-\frac{1}{2}}K^T K P^{-\frac{1}{2}})$.

Based on Schur complement lemma [36] and equation (31), the following conditions can be obtained,

$$\begin{bmatrix} -I & \sqrt{\eta}K \\ \sqrt{\eta}K & -u_{max}^2 P \end{bmatrix} \le 0 \tag{32}$$

For the system depicted by equation (10), it can be found that time-varying parameters $v_x, \frac{1}{v_x}, r$ and C_R are coupled in the system matrices. These parameters need to be processed before carrying out the design of RSC control law. Here, the polytope model method in [7] is applied to cover the range of time-varying parameters. Specifically, in this system, the longitudinal velocity is usually bounded. It can be assumed that v_x varies in the range of $[v_{xmin}, v_{xmax}]$, $\frac{1}{v_x}$ is bound in the range of $[\frac{1}{v_{xmax}}, \frac{1}{v_{xmin}}]$ and

v_{xmin}, v_{xmax} denote the minimum and maximum value of longitudinal velocity. Similarly, the same assumptions are imposed on r and C_R, namely, r and C_R vary in the range of $[r_{max}, r_{min}]$ and $[C_{Rmin}, C_{Rmax}]$, respectively. Therefore, the time-varying parameters $v_x, \frac{1}{v_x}, r$ and C_R can be expressed by a linear combination of the vertices as follows:

$$\begin{cases} v_x = \sum_{i=1}^{2} \rho_{1i}\, \sigma_{1i}, & \frac{1}{v_x} = \sum_{i=1}^{2} \rho_{2i}\, \sigma_{2i} \\ r = \sum_{i=1}^{2} \rho_{3i}\, \sigma_{3i}, & C_R = \sum_{i=1}^{2} \rho_{4i}\, \sigma_{4i} \end{cases} \tag{33}$$

where σ represents the vertices coordinates of the polytope and ρ means the weighting factors, which can be denoted as:

$$\begin{cases} \rho_{11} = \frac{v_{xmax} - v_x}{v_{xmax} - v_{xmin}},\ \rho_{12} = \frac{v_x - v_{xmin}}{v_{xmax} - v_{xmin}} \\ \rho_{21} = \frac{\frac{1}{v_{xmax}} - \frac{1}{v_x}}{\frac{1}{v_{xmax}} - \frac{1}{v_{xmin}}},\ \rho_{22} = \frac{\frac{1}{v_x} - \frac{1}{v_{xmin}}}{\frac{1}{v_{xmax}} - \frac{1}{v_{xmin}}} \\ \rho_{31} = \frac{r_{max} - r}{r_{xmax} - r_{xmin}},\ \rho_{32} = \frac{r - r_{min}}{r_{xmax} - r_{xmin}} \\ \rho_{41} = \frac{C_{Rmax} - C_R}{C_{Rmax} - C_{Rmin}},\ \rho_{42} = \frac{C_R - C_{Rmin}}{C_{Rmax} - C_{Rmin}} \end{cases}$$

$$\begin{cases} \sigma_{11} = v_{xmin},\ \sigma_{12} = v_{xmax} \\ \sigma_{21} = \frac{1}{v_{xmin}},\ \sigma_{22} = \frac{1}{v_{xmax}} \\ \sigma_{31} = r_{min},\ \sigma_{32} = r_{max} \\ \sigma_{41} = C_{Rmin},\ \sigma_{42} = C_{Rmax} \end{cases} \tag{34}$$

Combined equation (10) and equation (33), the system plant of trajectory tracking system can be rewritten in the polytypic form as:

$$\dot{x}(t) = \sum_{i=1}^{16} \beta_i \left[A_i x(t) + B_i u(t) + D_i(t)\right] \tag{35}$$

where $\beta_1 = \bar{\beta}_{1111}, \beta_2 = \bar{\beta}_{1112}, \cdots, \beta_{16} = \bar{\beta}_{2222}$, $\sum_{i=1}^{16} \beta_i = 1$ and $\bar{\beta}_{ijmn} = \sum_{i=1}^{2}\sum_{j=1}^{2}\sum_{m=1}^{2}\sum_{n=1}^{2} \rho_{1i}\rho_{2j}\rho_{3m}\rho_{4n}$.

Define $\beta = [\beta_1, \beta_2, \cdots \beta_{16}]^T$, $y = [r, e_y, e_\varphi, e_v]^T$ and the LPV model of trajectory tracking system can be expressed as:

$$\begin{cases} \dot{x}(t) = A(\beta)x(t) + B(\beta)u(t) + D(t) \\ y(t) = Cx(t) \end{cases} \tag{36}$$

with

$$C = \begin{bmatrix} 0 & 1 & 0 & 0 & 0 \\ 0 & 0 & 1 & 0 & 0 \\ 0 & 0 & 0 & 1 & 0 \\ 0 & 0 & 0 & 0 & 1 \end{bmatrix}$$

Then, the state-feedback controller is proposed as:

$$u(t) = K(\beta)x(t) = \sum_{i=1}^{16} \beta_i K_i x(t) \tag{37}$$

where K_i is the control gain, the key parameters need to be determined. Combined the equations (36) with (37), the closed-loop system can be obtained as

$$\begin{cases} \dot{x}(t) = \sum_{i=1}^{16} \beta_i \left[(A_i + B_i K_i)x(t) + D_i(t)\right] \\ y = Cx(t) \end{cases} \tag{38}$$

According to theorem 1and equation (38), if the following condition is fulfilled, the controller will achieve the aim of ensuring system stability and H_∞ performance index of the closed-loop system.

$$\begin{bmatrix} (A_i + B_i K_i)S + S^T(A_i + B_i K_i)^T & S^T C^T & I & P_i - S^T \\ * & -\gamma I & 0 & 0 \\ * & * & -\gamma I & 0 \\ * & * & * & 0 \end{bmatrix} < 0, i = 1,2,\cdots n$$

$$\begin{bmatrix} -I & \sqrt{\eta} K_i \\ \sqrt{\eta} K & -u_{max}^2 P_i \end{bmatrix} \le 0, i = 1,2,\cdots n \tag{39}$$

where the P_i is a symmetric positive definite matrix and S is a matrix with proper dimensions. γ represents the performance index of system in attenuating disturbance.

So far, the key to solve the trajectory tracking issue has converted to calculate the controller gain $K(\beta)$ by solving the inequality problems above. In this paper, we use the yalmip toolbox to solve this issue because it has simple syntax and is easy to use.

4 Comparative Test and Analysis for the Results from MPC and RSC

4.1 Platform Description and Test Setup

In this section, several simulation tests are carried out to compare the discrepancy of performance of the presented MPC and RSC control schemes, which are performed on the joint Carsim-Simulink platform with a high-fidelity and full-vehicle model. In this paper, we mainly compare their performance under the following test conditions respectively: 1) parameters uncertainties: mass, 2) sensors measurement error, 3) extreme driving condition: 90° Turn with big curvature. Besides, to quantify the tracking accuracy, the root mean square error (RMSE) is used in section 4.2 and section 4.3 and formula is given by

$$RMSE = \sqrt{\frac{1}{M}\sum_{i=1}^{m}(y_i - y_r)^2} \tag{40}$$

where M is the number of time periods, y_i is the measured output and y_r donates the reference output value. The vehicle and other related parameters used in simulation are listed in Table 2.

4.2 Parameters Uncertainties Case 1: Mass

Vehicle mass is a key parameter for the design of trajectory tracking controllers, which is varying when the number of passengers and cargo changes. In order to guarantee the

safety of AGVs, the tracking controllers must show robustness to varying parameters in the vehicle model. In this section, we carry out the test with different mass (i.e. m, $m + 30\%m$, $m - 30\%m$). Note that in this section, the main objective is to illustrate their robustness to mass uncertainties and a straight line is used as the reference path. In addition, the initial lateral, angular and velocity errors are set as -1m, 0, -2m/s, respectively.

The simulation results are shown in Figure 4 and the quantifying results are given by the Table 3. From Figure 4 (a) and (b), it can be seen that MPC-based controller shows a faster response than RSC-based one and shown that mass is a key parameter which can influence the response time, namely, the heavier the quality, the slower the response. As shown in Figure 4 (b) and (c), both controllers demonstrate their robustness to the mass uncertainty. The response results of lateral velocity and yaw rate are demonstrated in Figure 4 (d) and (e). Figure 4 (f) and (g) show the value of control variables and it can be concluded that RSC-based controller has a smoother variation than MPC-based control scheme. Furthermore, combined Figure 4 with Table 3, it can be known that both controllers can track the desired trajectory accurately in a limited time, while in terms of tracking accuracy, MPC performs better.

4.3 Parameters Uncertainties Case 2: Sensor Measurement Error

In this paper, although we assume that the system state can be measured through sensors, the measurement is may be inaccurate with errors. For instance, the lateral velocity is difficult to obtained exactly without expensive equipment like dual antenna GPS. Therefore, in this section, the lateral velocity is set to have -30%, 0, +30% errors compared to accurate values, so the controllers' performance of robustness to state variable uncertainties can be tested. The initial lateral, angular and velocity error are also set as -1m, 0, -2m/s, respectively. Similarly, the simulation results are shown in Figure 5 and the quantifying results are given by the Table 4. Figure 5 (a), (b) and (c) display the response results of lateral error, longitudinal velocity error and angular error, respectively. It can be seen that RSC-based controller demonstrates well robustness and the sensor noise has little effect on tracking performance, which can be also illustrated in Table 4. By contrast, MPC-based one shows that its performance can be interfered by measurement noise significantly, but it can adjust the control outputs in time by online optimization and track the desired trajectory in the end. Apparently, the MPC-based controller shows a faster response than RSC-based one like the results in Figure 5. Besides, according to Table 4, MPC displays a better tracking performance than RSC in all the test situations of lateral velocity measurement error. Figure 5 (d) and (e) display the response results of lateral velocity and yaw rate, respectively. It can be known that for MPC-based controller, the value of lateral velocity and yaw rate is bigger than that of RSC-based one, which is result from the faster response of tracking desired trajectory. Figure 5 (f) and (g) demonstrate the control outputs of both controllers.

Table 2 Vehicle and trajectory parameters used in controller design process

Definition	*Symbol*	*Value*
Vehicle mass	m	1750kg
Inertia moment of the vehicle about yaw axis	I_z	2500kg.m^2
Distance of the front/rear axle from CG	l_f/l_r	1.24m/1.46m
Nominal cornering stiffness of front/rear wheels	C_f/C_r	60kN/rad/60kN/rad
Minimal/Maximal longitudinal velocity	v_{min}/v_{max}	16m/s/30m/s
Minimal/Maximal yaw rate	r_{min}/r_{max}	-0.5rad/s/0.5rad/s
Minimal/Maximal curvature of the path	C_{Rmin}/C_{Rmax}	-0.02m^{-1}/0.02m^{-1}

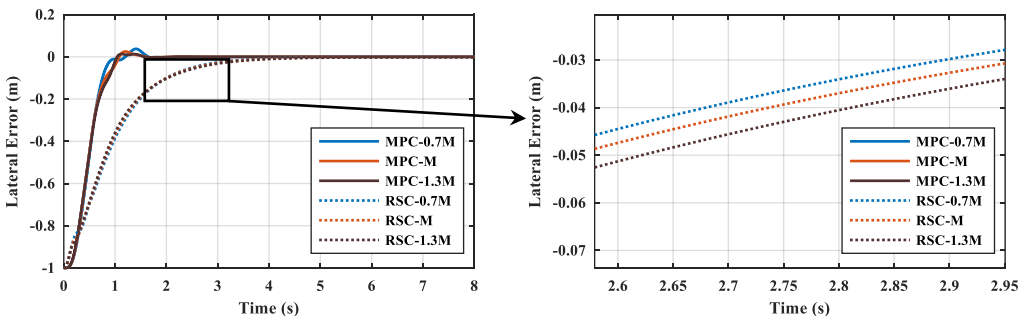

(a)

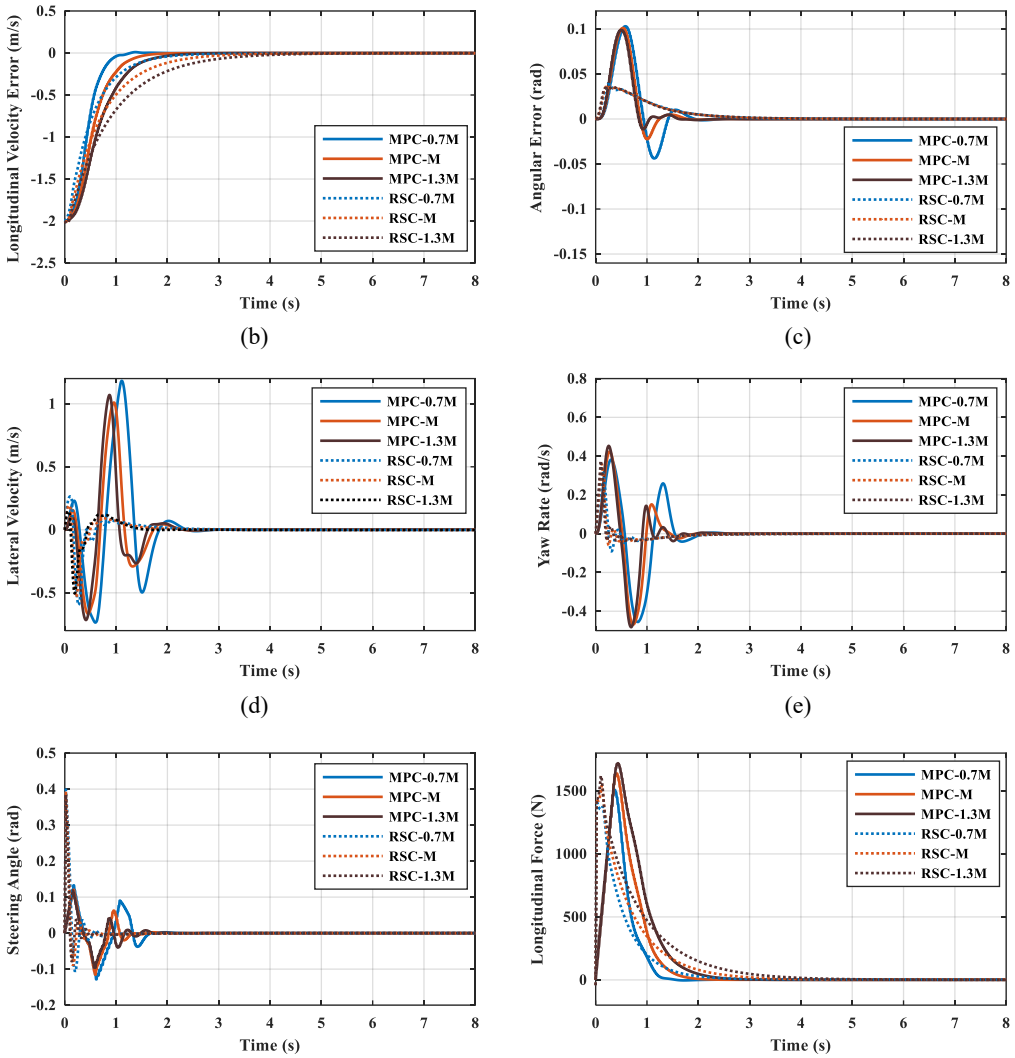

Figure 4 The simulation results of vehicle states in robust test for varying vehicle mass. (a) lateral error (b) longitudinal velocity errors (c) lateral velocity (d) yaw rate (e) angular error (f) steering angel (g) general longitudinal force.

Table 3 Test results for varying vehicle mass

	Model Uncertainties	*Sensor Measurement error*	*Road Adhesion*	*Maximum Curvature*	*Path Tracking Accuracy (REMS)*	*Velocity Tracking Accuracy (REMS)*
MPC	Mass (-30%)	None	0.8	0	0.030404	0.088650
	Mass (0%)				0.020603	0.121660
	Mass (+30%)				0.029750	0.146200
RSC	Mass (-30%)				0.041542	0.094962
	Mass (0%)				0.040154	0.122076
	Mass (+30%)				0.040738	0.149632

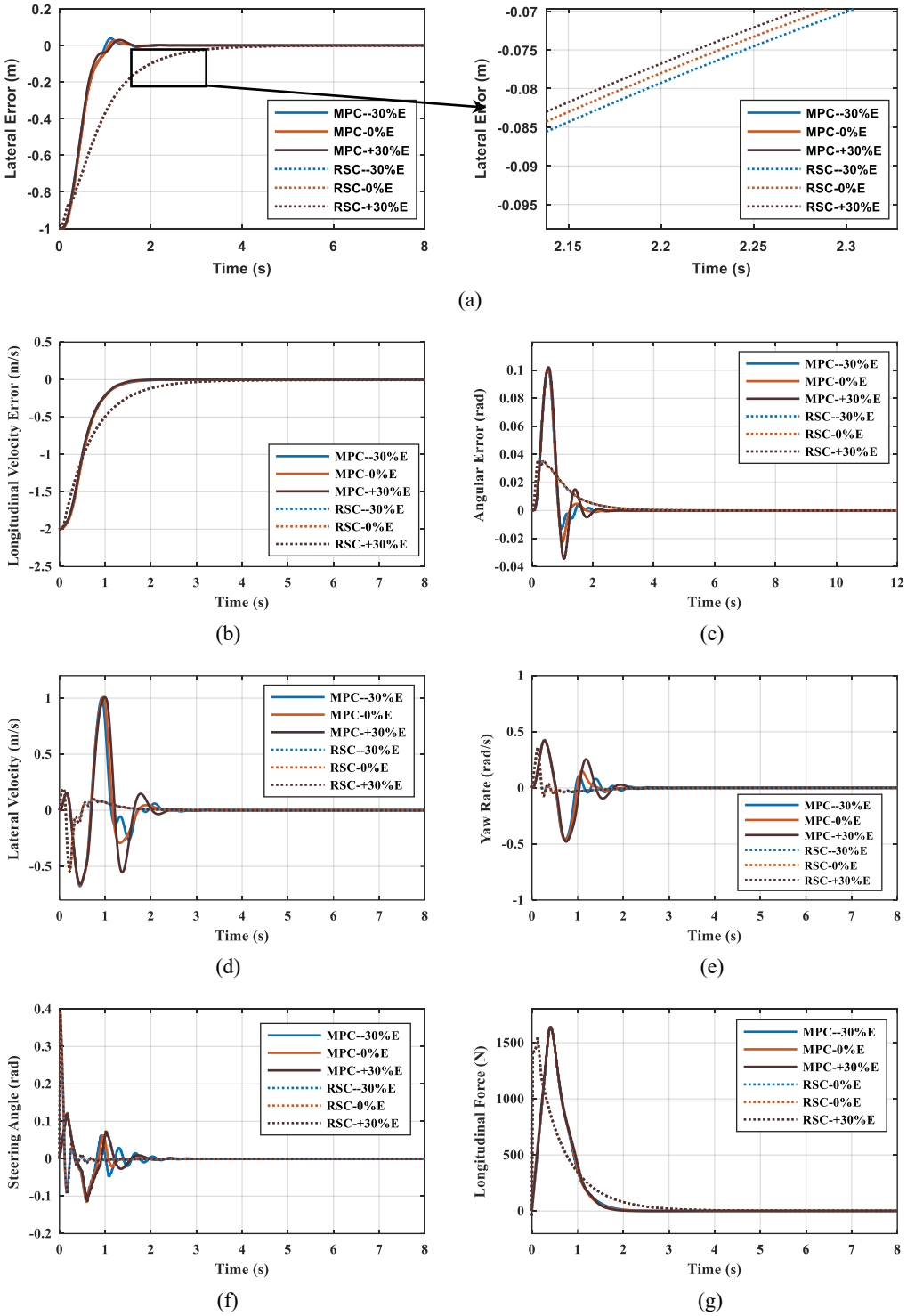

Figure 5 The simulation results of vehicle states in robustness test of lateral velocity measurement error. (a) lateral error (b) longitudinal velocity errors (c) lateral velocity (d) yaw rate (e) angular error (f) steering angel (g) general longitudinal force

Table 4 Test results for lateral velocity measurement error

	Model Uncertainties	*Sensor Measurement Error*	*Road Adhesion*	*Maximum Curvature*	*Path Tracking Accuracy (REMS)*	*Velocity Tracking Accuracy (REMS)*
MPC	None	-30% Lateral Velocity Error	0.8	0	0.028536	0.123840
		0			0.027948	0.119668
		+30% Lateral Velocity Error			0.028339	0.123798
RSC		-30% Lateral Velocity Error			0.041838	0.124630
		0			0.040754	0.120076
		+30% Lateral Velocity Error			0.040295	0.122228

4.4 Extreme Driving Condition: 90° Turn

In this section, with the purpose to obtain the maximum velocity that both controllers can perform under the given road conditions, the vehicle will execute 90° turn maneuverer and the maximum curve of the predefined path is $0.02m^{-1}$, which can be deemed as extreme road condition for vehicle to carry out. Besides, the road adhesion is set as 1 and the initial lateral, angular and velocity error are all set as zero. On the basis of vehicle dynamics [14], the longitudinal and lateral acceleration is subjected to road adhesion, namely,

$$\sqrt{a_x^2 + a_y^2} \leq \mu g \tag{41}$$

where a_x, a_y donate the longitudinal and lateral acceleration of vehicle, respectively. μ represents the road adhesion coefficient and g means the gravitational acceleration. Thus, it can be can assumed that if the acceleration of vehicle is close to μg, the vehicle is in critical state of out of control.

In this section, we increase the desired velocity continuously until the acceleration of vehicle is close to the μg, so as to obtain the critical velocity of the vehicle under MPC-based and RSC-based control algorithms. Figure 6 (a) and (b) show the simulation results of path tracking and vehicle acceleration. From the results, it can be found that the vehicle has reached nearly the critical state under both control schemes. Next, from Figure 7 (a) and (b), it can be seen that RSC-based trajectory tracking controller can reach the maximum velocity 22m/s while guaranteeing the stability of the system. However, the maximum velocity tracking error has reached 1.5m/s because there is slight side slip. The maximum desired velocity that MPC-based controller can follow is about 21m/s. If the desired velocity is further increased, the vehicle will experience a significant side slip and controller loses its tracking ability in the end. Figure 7 (c) and (d) demonstrate the lateral velocity and yaw rate of both controllers, which are dominated in an accepted range [26] and the control outputs is shown in Figure 7 (e) and (f).

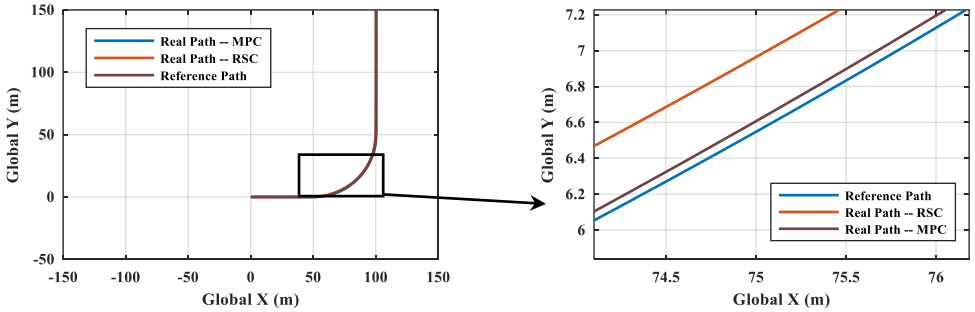

(a)

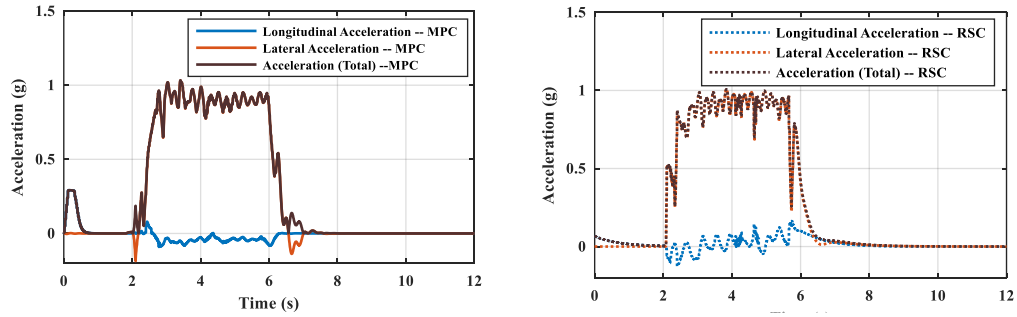

(b)

Figure 6 The simulation results of path tracking and acceleration in 90° Turn. (a) results of path tracking; (b) results of vehicle acceleration

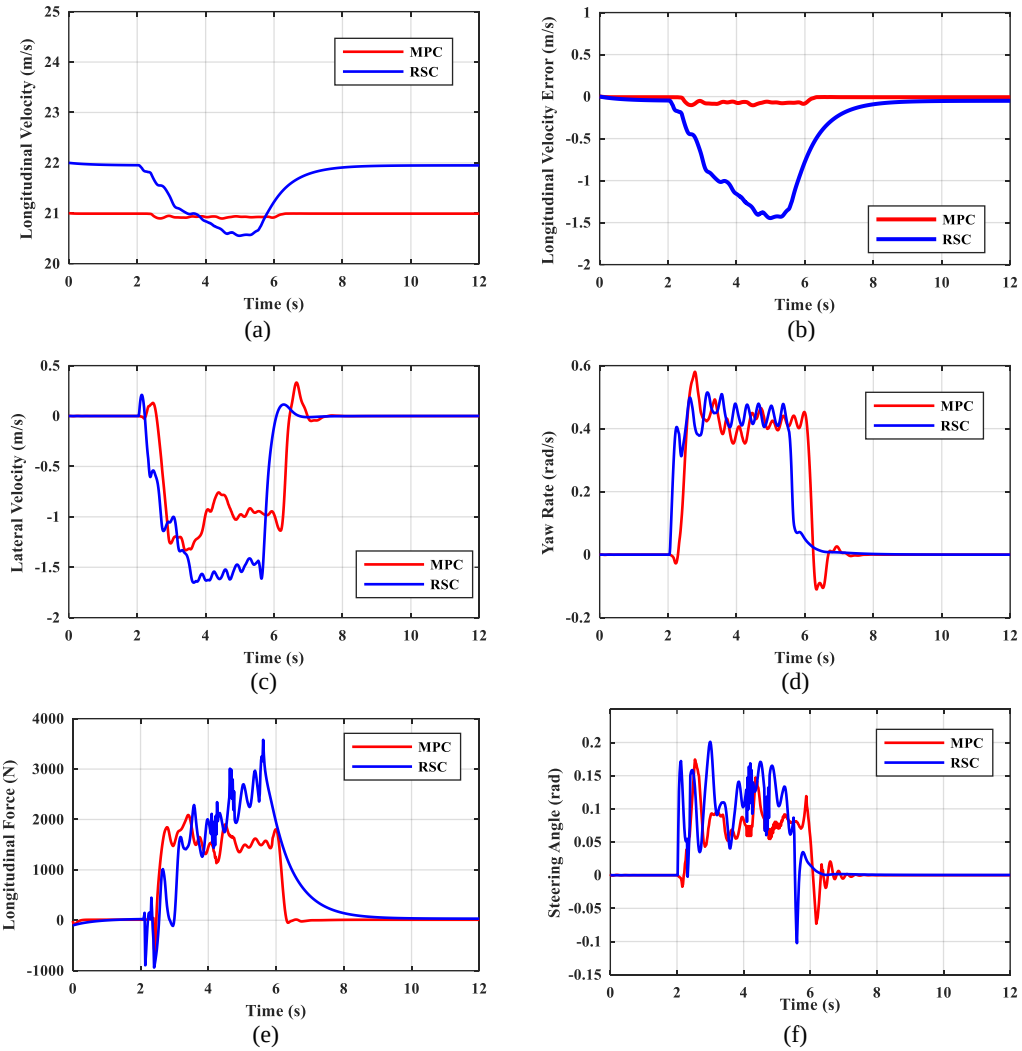

Figure 7 The simulation results of vehicle states in 90° Turn. (a) results of longitudinal velocity; (b) results of longitudinal velocity error; (c) results of lateral velocity; (d) results of yaw rate; (e) control outputs of longitudinal force; (f) control outputs of steering angle

5 Conclusions

In this paper, a comparative study of trajectory tracking control using MPC and RSC techniques of an automated vehicle is presented. First of all, the tracking model with 3-DOF (i.e. longitudinal-lateral-yaw) vehicle dynamic model and linear tire model is deduced. Then, based on the model predictive control theory and robust H_∞ control theory, the MPC-based and RSC-based trajectory tracking controller is proposed, respectively. This paper focuses on studying the tracking ability of MPC-based and RSC-based controllers and comparing the discrepancy between them under different scenarios. Therefore, the mass uncertainties, sensor measurement noise and the performance in extreme driving conditions: 90° turn with big curvature are considered. The simulation results show that mass uncertainty and sensor measurement noise of lateral velocity display little effect on RSC-based controller, while that put relatively greater influence on MPC-based one. But MPC-based controller shows a faster response speed and more accurate tracking performance than RSC-based controller. Finally, for the test of 90° turn with maximum curvature $0.02\ m^{-1}$, the maximum velocity that RSC-based controller can carry out has reached 22m/s, which is slightly better than MPC-based one: 21m/s.

6 Declaration

Acknowledgements

The authors sincerely thanks to Dr. Xin Yang of Chongqing University for his critical discussion and reading during manuscript preparation.

Funding

Supported by the State Key Laboratory of Mechanical System and Vibration(Grant No. MSV202016), and National Natural Science Foundation of China (Grant No. 51705044), and the State Key Laboratory of Mechanical Transmissions(Grant No. SKLMT-KFKT-201806).

Availability of data and materials

The datasets supporting the conclusions of this article are included within the article.

Authors' contributions

The author' contributions are as follows: Xiaolin Tang was in charge of the whole trial; Kai Yang wrote the manuscript; Yechen Qin, Yanjun Huang, Hong Wang and HuaYan Pu are assisted with sampling and laboratory analyses and checking.

Competing interests

The authors declare no competing financial interests.

Consent for publication

Not applicable

Ethics approval and consent to participate

Not applicable

References

[1] Howard, D., & Dai, D. (2014, January). Public perceptions of self-driving cars: The case of Berkeley, California. In Transportation research board 93rd annual meeting (Vol. 14, No. 4502, pp. 1-16).

[2] González, D., Pérez, J., Milanés, V., & Nashashibi, F. (2015). A review of motion planning techniques for automated vehicles. IEEE Transactions on Intelligent Transportation Systems, 17(4), 1135-1145.

[3] Katrakazas, C., Quddus, M., Chen, W. H., & Deka, L. (2015). Real-time motion planning methods for autonomous on-road driving: State-of-the-art and future research directions. Transportation Research Part C: Emerging Technologies, 60, 416-442.

[4] Badue, C., Guidolini, R., Carneiro, R. V., Azevedo, P., Cardoso, V. B., Forechi, A., ... & Veronese, L. (2019). Self-driving cars: A survey. *arXiv preprint arXiv:1901.04407*.

[5] Paden, B., Čáp, M., Yong, S. Z., Yershov, D., & Frazzoli, E. (2016). A survey of motion planning and control techniques for self-driving urban vehicles. IEEE Transactions on intelligent vehicles, 1(1), 33-55.

[6] Huang, Y., Wang, H., Khajepour, A., Ding, H., Yuan, K., & Qin, Y. (2019). A Novel Local Motion Planning Framework for Autonomous Vehicles based on resistance network and model predictive control. IEEE Transactions on Vehicular Technology.

[7] Hu, C., Jing, H., Wang, R., Yan, F., & Chadli, M. (2016). Robust H∞ output-feedback control for path following of autonomous ground vehicles. Mechanical Systems and Signal Processing, 70, 414-427.

[8] Peng, H., & Tomizuka, M. (1993). Preview control for vehicle lateral guidance in highway automation.

[9] Samuel, M., Hussein, M., & Mohamad, M. B. (2016). A review of some pure-pursuit based path tracking techniques for control of autonomous vehicle. International Journal of Computer Applications, 135(1), 35-38.

[10] Amer, N. H., Zamzuri, H., Hudha, K., Aparow, V. R., Kadir, Z. A., & Abidin, A. F. Z. (2018). Path tracking controller of an autonomous armoured vehicle using modified Stanley controller optimized with particle swarm optimization. Journal of the Brazilian Society of Mechanical Sciences and Engineering, 40(2), 104.

[11] Xu, S., & Peng, H. (2019). Design, analysis, and experiments of preview path tracking control for autonomous vehicles. IEEE Transactions on Intelligent Transportation Systems.

[12] Huang, Y., Ding, H., Zhang, Y., Wang, H., Cao, D., Xu, N., & Hu, C. (2019). A Motion Planning and Tracking Framework for Autonomous Vehicles Based on Artificial Potential Field Elaborated Resistance Network Approach. IEEE Transactions on Industrial

Electronics, 67(2), 1376-1386.

[13] Erlien, S. M., Fujita, S., & Gerdes, J. C. (2015). Shared steering control using safe envelopes for obstacle avoidance and vehicle stability. IEEE Transactions on Intelligent Transportation Systems, 17(2), 441-451.

[14] Rajamani, R. (2011). Vehicle dynamics and control. Springer Science & Business Media.

[15] Attia, R., Orjuela, R., & Basset, M. (2014). Combined longitudinal and lateral control for automated vehicle guidance. Vehicle System Dynamics, 52(2), 261-279.

[16] Borrelli, F., Falcone, P., Keviczky, T., Asgari, J., & Hrovat, D. (2005). MPC-based approach to active steering for autonomous vehicle systems. International Journal of Vehicle Autonomous Systems, 3(2), 265-291.

[17] Falcone, P., Borrelli, F., Asgari, J., Tseng, H. E., & Hrovat, D. (2007). Predictive active steering control for autonomous vehicle systems. IEEE Transactions on control systems technology, 15(3), 566-580.

[18] Ji, J., Khajepour, A., Melek, W. W., & Huang, Y. (2016). Path planning and tracking for vehicle collision avoidance based on model predictive control with multi-constraints. IEEE Transactions on Vehicular Technology, 66(2), 952-964.

[19] Ni, J., Hu, J., & Xiang, C. (2019). Robust path following control at driving/handling limits of an autonomous electric racecar. IEEE Transactions on Vehicular Technology, 68(6), 5518-5526

[20] Guo, J., Luo, Y., & Li, K. (2019). Robust gain-scheduling automatic steering control of unmanned ground vehicles under velocity-varying motion. Vehicle System Dynamics, 57(4), 595-616.

[21] Mayne, D. Q. (2014). Model predictive control: Recent developments and future promise. Automatica, 50(12), 2967-2986.

[22] Yakub, F., & Mori, Y. (2015). Comparative study of autonomous path-following vehicle control via model predictive control and linear quadratic control. Proceedings of the Institution of Mechanical Engineers, Part D: Journal of automobile engineering, 229(12), 1695-1714.

[23] Bemporad, A., & Morari, M. (1999). Robust model predictive control: A survey. In Robustness in identification and control(pp. 207-226). Springer, London.

[24] Mayne, D. Q., Rawlings, J. B., Rao, C. V., & Scokaert, P. O. (2000). Constrained model predictive control: Stability and optimality. Automatica, 36(6), 789-814.

[25] Falcone, P., Tufo, M., Borrelli, F., Asgari, J., & Tseng, H. E. (2007, December). A linear time varying model predictive control approach to the integrated vehicle dynamics control problem in autonomous systems. In 2007 46th IEEE Conference on Decision and Control (pp. 2980-2985). IEEE.

[26] Falcone, P., Borrelli, F., Asgari, J., Tseng, H. E., & Hrovat, D. (2007). Predictive active steering control for autonomous vehicle systems. IEEE Transactions on control systems technology, 15(3), 566-580.

[27] Falcone, P., Borrelli, F., Tseng, H. E., Asgari, J., & Hrovat, D. (2008, June). A hierarchical model predictive control framework for autonomous ground vehicles. In 2008 American Control Conference (pp. 3719-3724). IEEE.

[28] Wada, N., Tomosugi, H., & Saeki, M. (2013). Model predictive tracking control for a linear system under time-varying input constraints. International Journal of Robust and Nonlinear Control, 23(9), 945-964.

[29] Hu, C., Zhao, L., Cao, L., Tjan, P., & Wang, N. (2020). Steering control based on model predictive control for obstacle avoidance of unmanned ground vehicle. Measurement and Control, 0020294019878871.

[30] Wang, R., Jing, H., Hu, C., Yan, F., & Chen, N. (2016). Robust H∞ Path Following Control for Autonomous Ground Vehicles With Delay and Data Dropout. IEEE Transactions on Intelligent Transportation Systems, 17(7), 2042-2050.

[31] Zhang, H., Zhang, X., & Wang, J. (2014). Robust gain-scheduling energy-to-peak control of vehicle lateral dynamics stabilisation. Vehicle System Dynamics, 52(3), 309-340.

[32] Du, H., Zhang, N., & Naghdy, F. (2011). Velocity-dependent robust control for improving vehicle lateral dynamics. Transportation research part C: emerging technologies, 19(3), 454-468.

[33] Huang, X., Zhang, H., Zhang, G., & Wang, J. (2014). Robust Weighted Gain-Scheduling H∞ Vehicle Lateral Motion Control With Considerations of Steering System Backlash-Type Hysteresis. IEEE Transactions on Control Systems Technology, 22(5), 1740-1753.

[34] Liu, C., & Tomizuka, M. (2016). Geometric considerations on real time trajectory optimization for nonlinear systems. System & Control Letters, p. in review.

[35] Ren Yue. (2018). Research on Active Tracking and Collision Avoidance Control of Intelligent Electric Vehicles (in Chinese).

[36] Boyd, S., El Ghaoui, L., Feron, E., & Balakrishnan, V. (1994). Linear matrix inequalities in system and control theory (Vol. 15). Siam.

Biographical notes

Kai Yang, is currently pursuing the Ph.D. degree in the *Department of Automotive Engineering, Chongqing University, Chongqing, China*. He received the B.E. degree in vehicle engineering from *Wuhan University of Technology*, in 2018. His research interests include automated vehicles, motion planning and control.
E-mail: kaiyang0401@gmail.com

Xiao-Lin Tang, is currently an Associate Professor at the *Department of Automotive Engineering, Chongqing University,* Chongqing, China. He received the Ph.D. degree in Mechanical Engineering from *Shanghai Jiao Tong University*, *China*, in 2015.
E-mail: tangxl0923@cqu.eud.cn

Ye-Chen Qin, is currently working as an Associate Professor with the *Beijing Institute of Technology, China*. He received the B.Sc. and Ph.D. degrees in mechanical engineering from the *Beijing Institute of Technology, China*, in 2010 and 2016, respectively.
E-mail: qinyechenbit@gmail.com

Yan-Jun Huang, is currently a Research Associate at the Department of Mechanical and Mechatronics Engineering at *University of Waterloo*, where he received his PhD degree in 2016.
E-mail: y269huan@uwaterloo.ca

Hong Wang, is currently a Research Associate in mechanical and mechatronics engineering with the *University of Waterloo*. She received the Ph.D. degree from the *Beijing Institute of Technology, China,* in 2015.
E-mail: hong.wang@uwaterloo.ca

Hua-Yan Pu, is currently an Associate Professor at the State Key Laboratory of Mechanical Transmissions, Chongqing University.

She received the Ph.D. degree from the Huazhong University of Science and Technology, China, in 2011.
E-mail: phygood 2001@shu.edu.cn